J Mater Sci: Mater Med (2010) 21:2165–2173
DOI 10.1007/s10856-010-4077-6

Enhanced osteointegration of orthopaedic implant gradient coating composed of bioactive glass and nanohydroxyapatite

Xin-Hui Xie · Xiao-Wei Yu · Shao-Xian Zeng · Rui-Lin Du · Yu-Huai Hu · Zhen Yuan · Er-Yi Lu · Ke-Rong Dai · Ting-Ting Tang

Received: 7 December 2009 / Accepted: 29 March 2010 / Published online: 9 April 2010

Abstract We conducted histologic and histomorphometric studies to evaluate the osteointegration of gradient coatings composed of bioactive glass and nanohydroxyapatite (BG–nHA) on titanium-alloy orthopaedic implants and surrounding bone tissue in vivo. Titanium-alloy implants with a gradient coating (gradient coating group), uncoated implants (uncoated group), and implants with a conventional hydroxyapatite (HA) coating (HA coating group) were randomly implanted in bilateral femoral condyles of 36 male New Zealand rabbits. The bone–implant contact at 12 and 24 weeks and the new bone volume in the notch created for observing bone ingrowth at 4, 12, and 24 weeks were found greater in the gradient coating group than those in both the uncoated group and the HA coating group ($p < 0.05$). Fluorescence micrographs showed active osteogenesis in the gradient coating group at 4 weeks after implantation. These findings indicated that BG–nHA gradient coatings could enhance the osteointegration of orthopaedic implant.

Xin-Hui Xie, Xiao-Wei Yu are Co-first authors with equal contribution to this work.

X.-H. Xie · X.-W. Yu · Z. Yuan · K.-R. Dai · T.-T. Tang (✉)
Department of Orthopedic Surgery, Shanghai Ninth People's Hospital, Shanghai Jiao Tong University School of Medicine, Shanghai, China
e-mail: tingtingtang@hotmail.com

E.-Y. Lu
Department of Prosthodontics, Shanghai Ninth People's Hospital, Shanghai Jiao Tong University School of Medicine, Shanghai, China

S.-X. Zeng · R.-L. Du · Y.-H. Hu
Chinese Academy of Sciences, Shanghai Institute of Ceramics, Shanghai, China

1 Introduction

Hydroxyapatite (HA) is osteoconductive and has been widely used as a coating on metallic orthopaedic implants to improve osteointegration between implants and bone [1–3]. Conventional plasma spraying is now the most widely used technique to produce a HA coating on titanium alloy (Ti–6Al–4 V) [4, 5]. Although this process is inexpensive and quick, there are multiple drawbacks caused by the high temperature at which it is done, including low and varying bond strength with the metal substrate and some decomposition to soluble calcium phosphate compounds [6–8]. Delamination of the coating is usually induced by residual stress arising from the mismatch of the coefficient of the thermal expansion between the titanium alloy and the HA coating [7, 9]. These shortcomings damage the bone–prosthesis interface, which could result in long-term prosthesis instability [1]. Although Capello et al. [10] proves that both the femoral aseptic revision and mechanical failure rates are 0.6% at 15-year minimum follow up, peoples are still developing various methods to optimize the artificial prosthesis.

Using sintering technology at a temperature lower than 800°C, we added a functional gradient coating composed of bioactive glass (BG) and nano-HA composite ceramic to the titanium alloy, wherein the nano-HA concentration was gradually increased from the innermost layer to the outmost layer. The pure BG had contact with the alloy substrate, and the coating surface was composed of pure nanohydroxyapatite (nHA). BG has an excellent bioactive nature that promotes bone formation, and its thermal expansion coefficient can be controlled to match that of titanium alloy [11–13]. Nanophase ceramics have been proved to enhance osteoblast function and have the potential to enhance osteointegration of orthopaedic implants and thus improve

overall implant efficacy [14–17]. The present work was undertaken to develop a novel coating capable of adhering firmly to titanium alloy and forming nanohydroxyapatite layer at the surface of coating to promote the bone formation. We have proved previously that the gradient coating had a high bonding strength to titanium alloy and the good compatibility to support the attachment and the growth of human bone marrow mesenchymal stem cells [18–20]. Thus, it is expected that proper design of this multi-component coatings will further enhance their application in the biomedical field. In this study, we evaluated the effect of osteointegration of BG–nHA-coated titanium alloy (Ti–6Al–4 V) implants by comparing with that of the conventional HA-coated and uncoated implants in vivo.

2 Materials and methods

2.1 Coatings and implants

Commercially available titanium-alloy cylinders 15 mm long and 2.5 mm in diameter were prepared for implantation by creating a notch of 1.0 mm wide and 1.0 mm deep along their long axis (Fig. 1). The notch was designed to allow observations of bone ingrowth and remodeling. The coatings were prepared by sintering technology at a temperature 800°C according to our previous method [19]. The titanium alloy was treated with sandblasting before coating, so that the metal surface became rough and was conducive to the combination between the metal substrate and the coating. Nanohydroxyapatite and bioactive glass composite powders were mixed according to the ratio of 0:10, 2:8, 3:7, 4:6, 5:5, 7:3, 8:2 and 10:0 [21], followed by spraying layer-by-layer on the titanium surface with varying ratios of concentration and then sintering at 800°C to form a gradient coating. After that, the surface and a cross section of the coating were observed by scanning electron microscopy (SEM) and energy-dispersive spectrometer (EDS) (JSM-6700F, JEOL Ltd, Tokyo, Japan). Implants of the same shape and design were also prepared without coating (sandblasted in surface) and with a conventional plasma-sprayed HA coating to serve as controls.

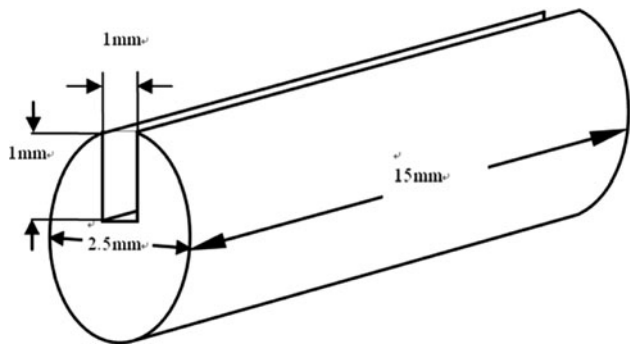

Fig. 1 Each titanium-alloy cylinder with a 1.0 mm-wide, 1.0 mm-deep notch along the long axis of the prothesis

2.2 Animal model

Thirty-six male New Zealand rabbits weighing an average of 3 kg were obtained from a licensed vendor (Shanghai Agricultural College, Shanghai, China). The animal experiment was approved by the local Animal Care Committee of the Shanghai Ninth People's Hospital. The rabbits were anesthetized and placed in the supine position. After the bilateral distal femoral condyles were surgically exposed, the medial and lateral condyles were drilled with 3.0 mm-diameter stainless steel drill bits, which formed a 3 mm-diameter, 15 mm-long horizontal bone tunnel vertical to the long axis of the femur. We randomly inserted 24 titanium-alloy implants with BG–nHA gradient coatings, 24 implants with conventional HA coatings, and 24 titanium-alloy implants without coatings into the holes on the bilateral femoral condyles of all the rabbits, resulting in a total of 72 implants. The wounds were carefully sutured.

After the surgeries were completed, the rabbits were hosted in cages and allowed case activities. At the following time intervals of 2, 4, 12, and 24 weeks after implantation, nine rabbits were sacrificed, thus six implants per time point for the BG–nHA gradient coatings and six implants per time point for the HA-coatings and uncoated implants were obtained for evaluations (Table 1). At 15 days and at 3 days before sacrificing animals, the fluorescence tracer tetracycline hydrochloride (Sigma, St Louis, MO, USA) was intraperitoneally injected with 30 mg/kg for labeling newly mineralized bone or new bone formation [22]. The femoral condyles with implants were harvested for radiography prior to fixation in 10% formalin solution.

2.3 Histology and histomorphometry analysis

The femoral condyles with the implants were processed for embedding in methylmethacrylate resin as described by Guglielmotti et al. [23]. The resin blocks were cut using a diamond saw (SP1600 Leica AG, Solms, Germany) into

Table 1 Experiment models and sample number in different groups at four time points after implantation

Groups	Time point (weeks)			
	2	4	12	24
Uncoated group	n = 6	n = 6	n = 6	n = 6
HA coating group	n = 6	n = 6	n = 6	n = 6
BG–nHA coating group	n = 6	n = 6	n = 6	n = 6

200 μm undecalcified sections, perpendicular to the implant. The cross sections were grounded and polished to a thickness of about 50 μm. They were examined by fluorescence microscopy (DM 4000B, Leica) before van Gieson staining. The bone–implant contact and the new bone volume within the notch was determined using an image analysis system (Bioquant Osteo, Nashville, TN, USA) on the stained sections. Six sections per implant were used for histomorphometric analysis. The sections from the specimens obtained at 12 weeks after implantation were also observed by SEM to evaluate interface bonding.

2.4 Statistical analysis

The bone–implant contact and the new bone volume were expressed as mean ± standard deviation (SD). Results were statistically evaluated by one-way analysis of variance, and pair-wise multiple comparisons were also performed using the least-significant difference, with the level of significance considered to be $p < 0.05$.

3 Results

3.1 Characteristics of the BG–nHA gradient coating

SEM showed that the surface of the BG–nHA gradient coating was composed of round shape crystals with a diameter of about 100 nm (Fig. 2, A1, A2). X-ray diffraction (XRD) analyses showed that these crystals were HA and no other crystal phase was detected (Fig. 2, A3). The SEM micrograph of the cross section (Fig. 2, B1, B2) showed that the thickness of the coating was about 120 μm, and the thickness of the coating was adjustable according the requirements. The middle layer of the coating was porous, but the interface between the coating and alloy was dense, and no cracks were found at the interface between titanium alloy and coating. EDS analyses (Fig. 2, B3) showed that the elements of Si and O in the coating had diffused into the alloy and formed a Ti–Al–V–Si–O layer on the surface of the alloy. The percentage of Ca and P increased with the distance close to the outer surface of the coating.

3.2 Radiographic and histological appearance

Radiographs indicated that all implants were well positioned at the femoral condyles and there were no translucent areas could be found (Fig. 3).

Fluorescence micrographs (Figs. 4, 5, 6, 7) showed fluorescence labeling, which indicated the active new bone formation around the implant at 2, 4, 12, and 24 weeks after implantation. Labeling was most dominant in the BG–nHA gradient at 4 weeks after implantation (Fig. 5).

New trabecular bone has formed around the implants and in the notch for all groups by 2 weeks after implantation under light microscope (Fig. 4). Within the notch, the new formed bone concentrated at the lateral area and the wall of the notch. The bone volume in BG–nHA coating group was higher than that in uncoated group, but there was no difference found between BG–nHA coating group and HA coating group. Figures 5 and 6 showed that bone contact with the implants increased gradually with

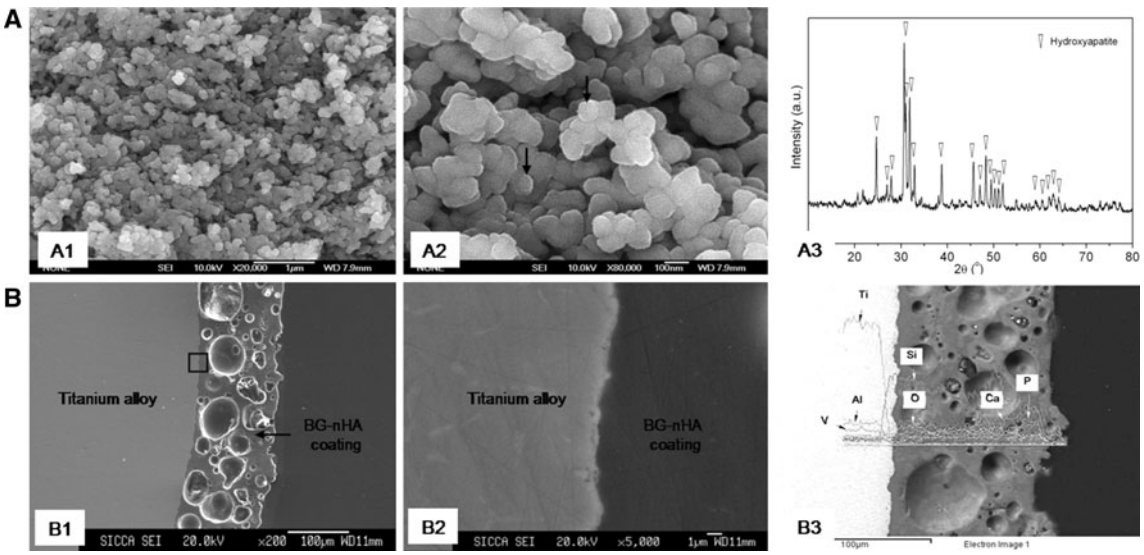

Fig. 2 SEM micrograph of the surface of the BG–nHA gradient coating (*A1* ×20000; *A2* ×80000). The surface is composed with round shape nano crystals and the diameter of crystal is about 100 nm (*arrows* in *A2*). XRD pattern of the coating (*A3*) shows that the crystals are HA, and no other crystal phase was detected. SEM micrograph of the cross section of the BG–nHA gradient coating (*B1* ×200, frame was magnified to *B2*; *B2* ×5000). EDS analysis of the cross section of the BG–nHA gradient coating (*B3*)

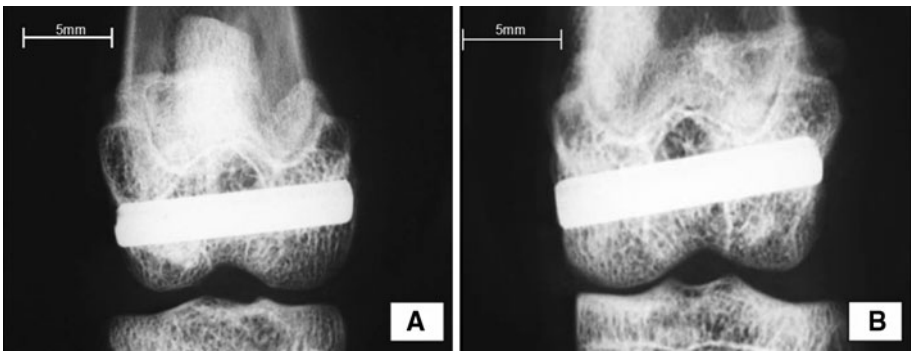

Fig. 3 X-ray photograph of the BG–nHA gradient coated prosthesis in rabbit. **a** 2 weeks after implantation, **b** 12 weeks after implantation

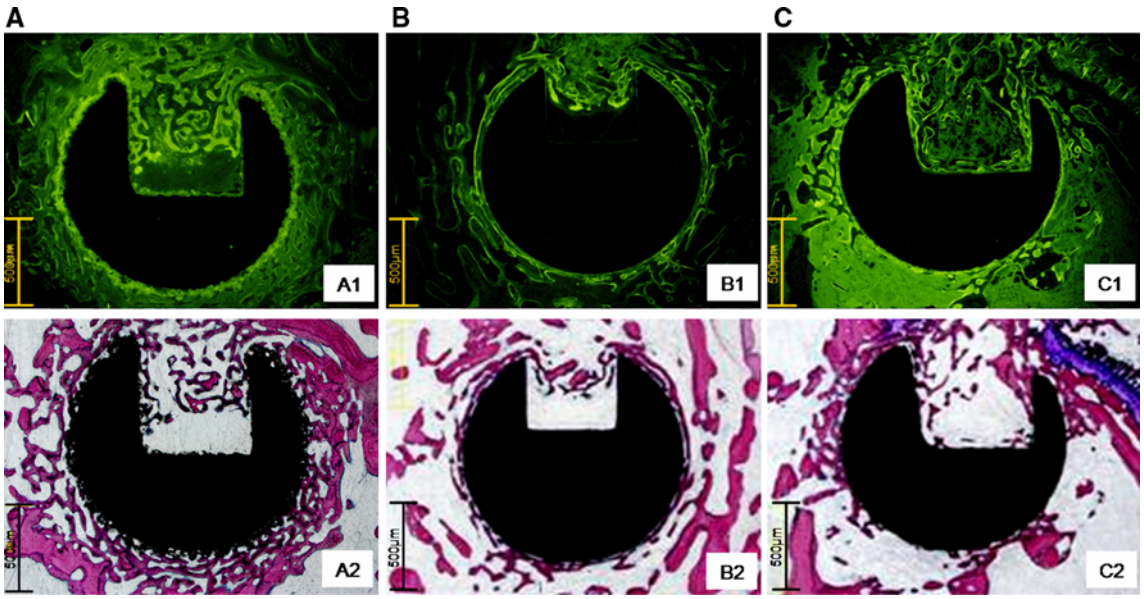

Fig. 4 Micrographs of undecalcified sections at week 2 after implantation showing the trabecular bone newly formed around the implants and in the notch in all the groups: **a** BG–nHA (bioactive glass, nanohydroxyapatite) gradient coating group, **b** uncoated group, **c** HA (hydroxyapatite) coating group. *A1*, *B1*, and *C1* are fluorescence micrographs. *A2*, *B2*, and *C2* are van Gieson–stained micrographs (×40)

time from 4 to 12 weeks and that most of the new bone at the lateral and central area of the notch was disappeared at 4 weeks after surgery in three groups. Most of the new bone was remained along the wall of the notch in three groups, but it was obvious that the bone volume in notch of the BG–nHA coating group was higher than that of other two groups, especially at 12 weeks (Fig. 9). Even being observed for 24 weeks after implantation (Fig. 7), the bone–implant contact in the BG–nHA coating group was most apparent among three groups. The trabecular bone around the implants had remodeled into lamellar bone in all groups. The newly formed bone could be hardly observed in notch of the HA coating group and uncoated group while that in the BG–nHA coating group was obvious along the wall of the notch.

SEM showed that at 12 weeks after implantation, there was good bonding at the coating-substrate interface in both the BG–nHA coating group and the HA coating group (Fig. 8a, c). The bone bonding in the uncoated group was poor, and there was spacing at the bone–implant interface in this group (Fig. 8b).

3.3 Histomorphometric parameters

As shown in Fig. 9, the average percentage bone–implant contact in each of the three groups increased gradually from 2 to 24 weeks; it was significantly higher in the BG–nHA coating group than that of both the HA coating group and the uncoated group at 12 and 24 weeks ($p < 0.05$). New bone volume in the notch in the HA coating group and the uncoated group decreased gradually from 2 to 24 week (Fig. 10); the volume at 4, 12, and 24 weeks for those groups was significantly lower than for the BG–nHA coating group ($p < 0.05$).

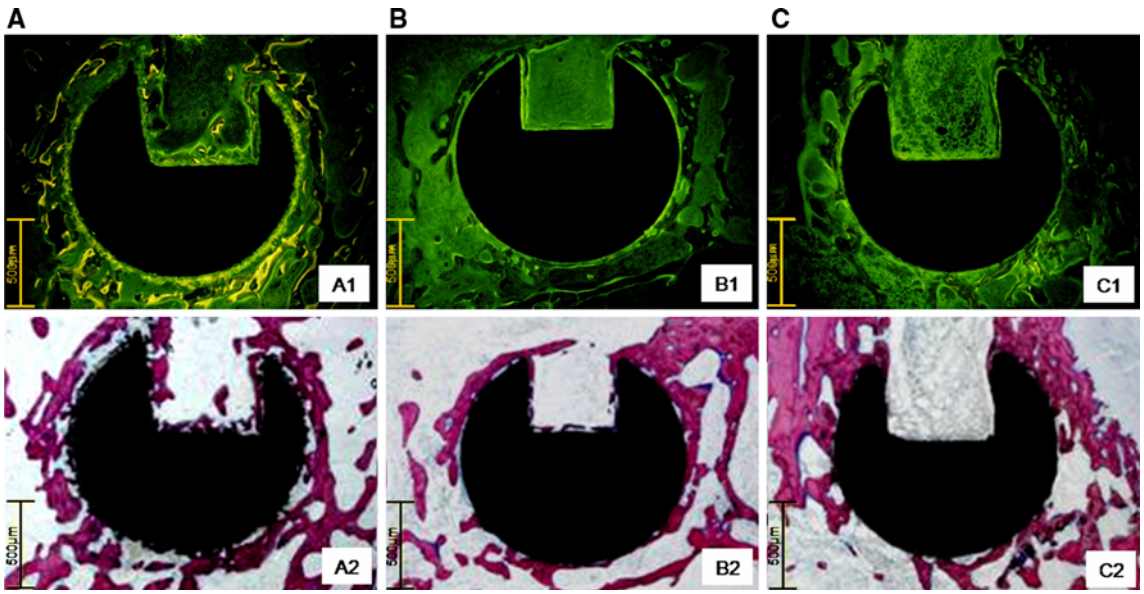

Fig. 5 Micrographs of undecalcified sections at week 4 after implantation, showing trabecular bone contact with implants. Some new bone remained in the notch of the BG–nHA (bioactive glass, nanohydroxyapatite) coating group, whereas most of the new bone in the notch disappeared in the uncoated group and in the HA (hydroxyapatite) coating group. Fluorescence labeling is most dominant in the BG–nHA gradient group. **a** BG–nHA gradient coating group, **b** uncoated group, **c** HA coating group. *A1*, *B1*, and *C1* are fluorescence micrographs. *A2*, *B2*, and *C2* are van Gieson–stained micrographs (×40)

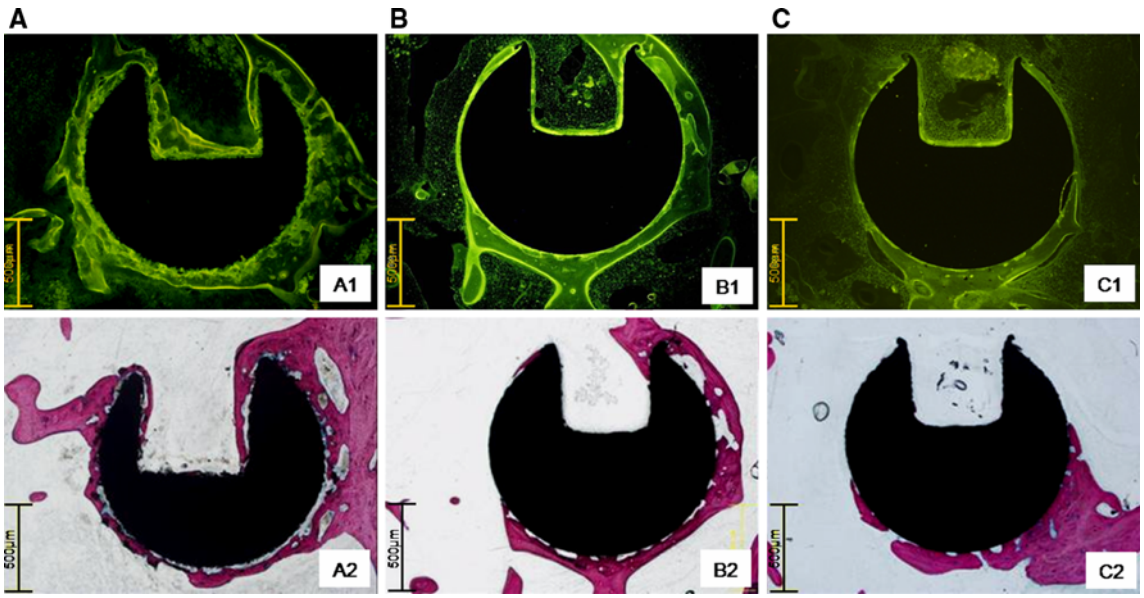

Fig. 6 Micrographs of undecalcified sections at 12 weeks after implantation, showing bone contact with implants. New bone remained in the notch in the BG–nHA (bioactive glass, nanohydroxyapatite) coating group, whereas most of the new bone in the notch disappeared in the uncoated group and the HA (hydroxyapatite) coating group. **a** BG–nHA gradient coating group, **b** uncoated group, **c** HA coating group. *A1*, *B1*, and *C1* are fluorescence micrographs. *A2*, *B2*, and *C2* are van Gieson–stained micrographs (×40)

4 Discussions

Modification of the surface of metallic implants is considered to benefit their biologic fixation which allows forming linkage between implant and living tissues. Metallic implants which are not bioactive tend to form a layer of fibrous tissue at the interface between the implant and bone. Conventional HA coating has been investigated by many researchers and has been clinically used as a reasonable method for increasing implant osteointegration [24–26]. However, delamination and resorption of the coating may result in prosthesis failure in retrospective

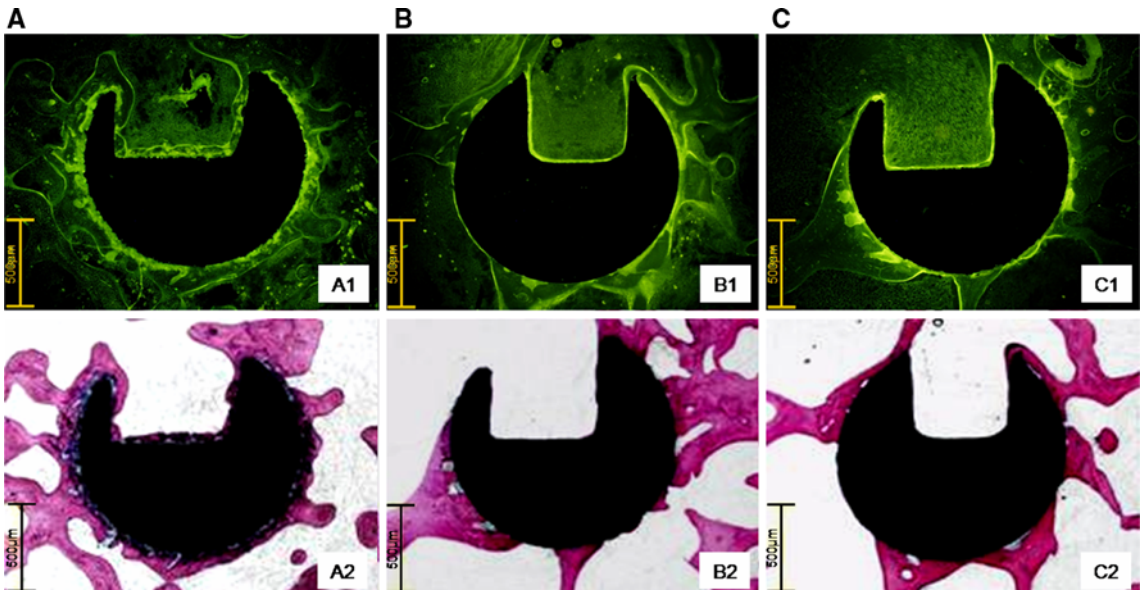

Fig. 7 Micrographs of undecalcified sections at week 24 after implantation, showing lamellar bone contact with implants. **a** BG–nHA (bioactive glass, nanohydroxyapatite) gradient coating group, **b** uncoated group, **c** HA coating group. *A1*, *B1*, and *C1* are fluorescence micrographs, *A2*, *B2*, and *C2* are van Gieson–stained micrographs (×40)

clinical studies [27, 28]. In order to improve the performance of orthopaedic implants, many researchers have attempted to optimize coatings by adding materials such as titanium powder, titanium oxide, zirconium oxide, Co–Cr–Mo alloy, or biphasic calcium phosphate [29–33]. In an early study, we used a BG–nHA composite to create a gradient coating by sintering it at temperatures lower than 800°C. We were of the opinion that the bioactive gradient coating was capable of improving the interfacial bonding between dissimilar solids, minimizing thermal stresses, reducing the effective driving force that could result in fracture, arresting cracks, and increasing long-term stability in the physiologic environment [34]. We found that the bond between the gradient coating and the titanium-alloy substrate was strong even after impact with a diamond saw during sample processing [19]. Moreover, bone bond directly with gradient coating and HA coating observed with SEM in present study.

The function of nanophase ceramic grains <100 nm in diameter is only partially understood. Compared with conventional ceramic formulations, the enhanced adhesion and proliferation of mesenchymal stem cells (MSCs) and osteoblasts has been observed with nanophase ceramic [35, 36]. Li [37] found that nanoapatite coatings was capable of promoting bone formation and direct bone apposition in bone chambers implanted into the lateral metaphysis of the distal femur of skeletally mature large coonhounds. Lewandrowski et al. analyzed the bioactivity of a nanohydroxyapatite-augmented, bioresorbable bone graft substitute made from an unsaturated polyester, poly(propylene fumarate), by evaluating the biocompatibility and osteointegration of implants placed into a rat tibial defect. They found that there was more reactive new bone formation in a group receiving the nanohydroxyapatite-augmented substitute than in a group receiving a microhydroxyapatite substitute [38]. In the present study, we found that the bone–implant contact in group with the BG–nHA coating implant was greater than that in HA coating group, especially at 12 and 24 weeks after implantation, implying that the nano-HA surface might contribute to the long-term biologic fixation of implants.

BG is a good osteoconductive ceramic and has been found to favor osteoblast growth and its differentiation [39–41]. Hench and Polak [42] reported that surface reactions of BG facilitated the release of soluble silicon, calcium, phosphorus, and sodium ions that gave rise to both intracellular and extracellular responses at the interface of the glass with its cellular environment. Researchers also found that BG dissolution products exerted genetic control over the osteoblast cycle, leading to differentiation and proliferation of bone cells and the expression of genes that regulated osteogenesis and production of growth factors [43, 44]. In our current experiment, we observed similar phenomena with new bone formation in the notch of three kinds of implants at 2 weeks after implantation; new bone volume in the BG–nHA coating group was higher than in the other two groups at 4, 12, and 24 week after implantation. The volume of the new bone formed in the notch in the HA coating group and the uncoated group decreased with time, and little was found at week 24 after implantation, which might be related to the stress-shielding effect [45]. According to Wollf's law, bone tissue adapts itself to the mechanical environment [46]. The bone tissue at the

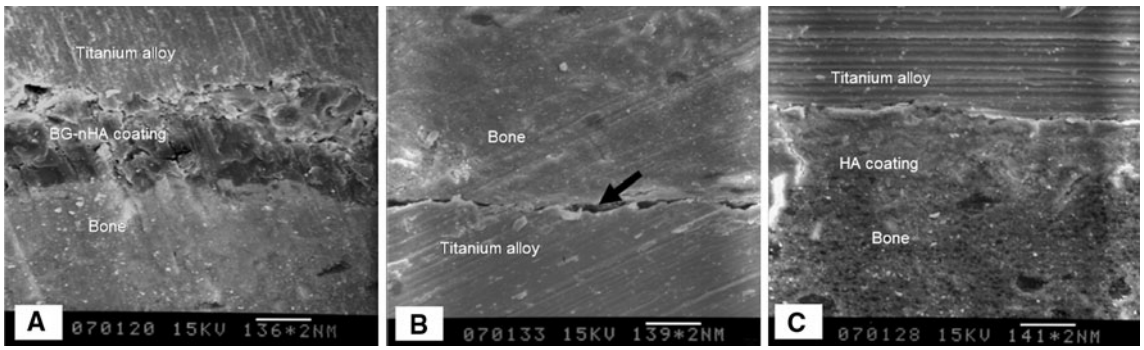

Fig. 8 Scanning electron micrographs of the bone–implant interface at week 12 after implantation (1000×). The interfaces in both **a** the BG–nHA (bioactive glass, nanohydroxyapatite) coating group, **b** the gap (*arrow*) is obvious found between bone and uncoated implant and **c** the HA coating group do not show good bonding

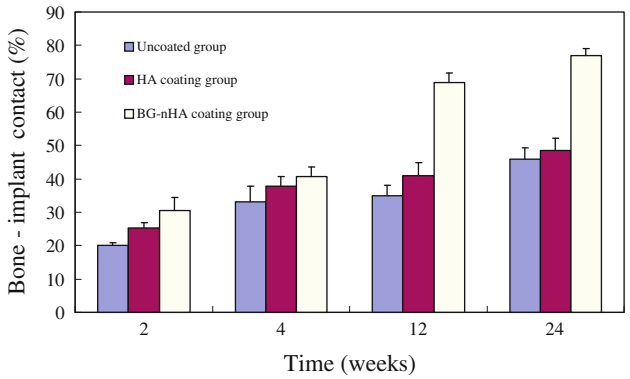

Fig. 9 Average bone–implant contact ratio at week 2, 4, 12, and 24 after implantation. Contact percentage in the BG–nHA (bioactive glass, nanohydroxyapatite) coating group is significantly higher than in the HA (hydroxyapatite) coating group and the uncoated group at week 12 and 24 after implantation ($p < 0.05$). Data are expressed as the mean ± standard deviation

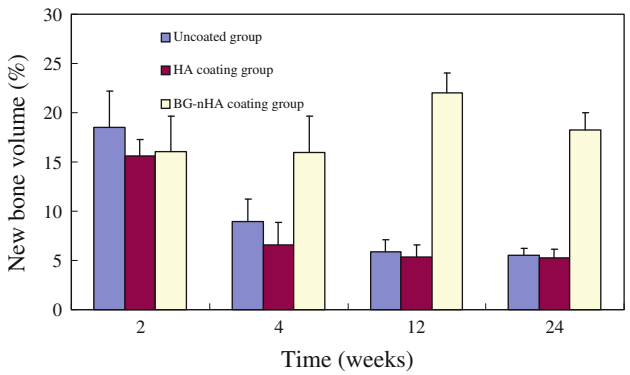

Fig. 10 The average new bone volume in the notch at week 4, 12, and 24 after implantation is significantly higher in the BG–nHA (bioactive glass, nanohydroxyapatite) coating group than in both the HA (hydroxyapatite) coating group and the uncoated group ($p < 0.05$). Data are expressed as the mean ± standard deviation

lateral and central area of the notch absorbed gradually because of lack of stress stimuli in three groups. The soluble ions released from the coating observed in the current study might stimulate the new bone formation and subsequently compensate the adverse effect due to potential stress-shielding, so we still found more bone at the area along the wall of the notch until 24 weeks. This suggested that the gradient coating could keep the bone volume around itself for a longer time, in favor of maintaining implant stability.

We were surprised to find that the percentage of bone–implant contact in the HA coating group was not statistically different from that in the uncoated group, different to what was reported by others [47, 48]. SEM at a magnification of 1000 showed that the HA coating in our study bonded tightly with bone but that there was a gap between uncoated implants and bone. bone–implant contact was determined on histological photographs at a magnification of 40 times, which was rather too low to reveal such a small gap. Therefore, we believed that the quality of the bone–HA coating bond was superior to that of the bone to uncoated implants as described previously by many researchers [1–3]. Further biomechanical studies are needed to compare the osteointegration and stability of these three kinds of implants in vivo.

5 Conclusions

Based on the findings of the present study, we believed that the BG–nHA gradient coating was bioactively able to enhance implant osteointegration by promoting bone formation and delaying the bone absorption around the materials, implying its beneficial effects on enhancement of biologic prosthesis fixation over long-term.

Acknowledgments We thank Prof. Ling Qin (The Chinese University of Hong Kong) for providing valuable editorial assistance. This research was supported by grants 0552nm024, 054119564 and 0852nm07200 from the Shanghai Science and Technology Development Fund, Shanghai Leading Academic Discipline Project (S30206), a grant from the Shanghai Shuguang Educational Funding

Committee and program for Shanghai Key Laboratory of Orthopaedic Implant (08DZ2230330) and Natural Science Foundation of Jiangsu province (No. BK2009449).

References

1. Gallo J, Landor I, Cechova I, Jahoda D. Comparison of hydroxyapatite-coated stems in total hip arthroplasty after a minimum 10-years follow-up. Acta Chir Orthop Traumatol Cech. 2008;75(5):339–46.
2. Shetty AA, Slack R, Tindall A, James KD, Rand C. Results of a hydroxyapatite-coated (Furlong) total hip replacement: a 13–15-year follow-up. J Bone Joint Surg Br. 2005;87(8):1050–4.
3. Wei M, Ruys AJ, Swain MV, Milthorpe BK, Sorrell CC. Hydroxyapatite-coated metals: interfacial reactions during sintering. J Mater Sci. 2005;16(2):101–6.
4. Rakngarm A, Mutoh Y. Characterization and fatigue damage of plasma sprayed HAp top coat with Ti and HAp/Ti bond coat layers on commercially pure titanium substrate. J Mech Behav Biomed Mater. 2009;2(5):444–53.
5. Chen CC, Huang TH, Kao CT, Ding SJ. Characterization of functionally graded hydroxyapatite/titanium composite coatings plasma-sprayed on Ti alloys. J Biomed Mater Res B Appl Biomater. 2006;78(1):146–52.
6. Kweh SW, Khor KA, Cheang P. An in vitro investigation of plasma sprayed hydroxyapatite (HA) coatings produced with flame-spheroidized feedstock. Biomaterials. 2002;23(3):775–85.
7. Liu X, Chu PK, Ding C. Surface modification of titanium, titanium alloys, and related materials for biomedical applications. Mater Sci Eng R Rep. 2004;47(3–4):49–121.
8. Heimann RB. Thermal spraying of biomaterials. Surf Coat Tech. 2006;201(5):2012–9.
9. Kurzweg H, Heimann RB, Troczynski T. Adhesion of thermally sprayed hydroxyapatite-bond-coat systems measured by a novel peel test. J Mater Sci. 1998;9(1):9–16.
10. Capello WN, D′Antonio JA, Jaffe WL, Geesink RG, Manley MT, Feinberg JR. Hydroxyapatite-coated femoral components: 15-year minimum follow-up. Clin Orthop Relat Res. 2006;453:75–80.
11. Kokubo T, Ito S, Sakka S, Yamamuro T. Formation of a high-strength bioactive glass-ceramic in the system MgO–CaO–SiO2–P2O5. J Mater Sci. 1986;21(2):536–40.
12. Peddi L, Brow RK, Brown RF. Bioactive borate glass coatings for titanium alloys. J Mater Sci. 2008;19(9):3145–52.
13. Moritz N, Vedel E, Ylanen H, Jokinen M, Hupa M, Yli-Urpo A. Characterisation of bioactive glass coatings on titanium substrates produced using a CO_2 laser. J Mater Sci. 2004;15(7):787–94.
14. Webster TJ, Ergun C, Doremus RH, Siegel RW, Bizios R. Enhanced functions of osteoblasts on nanophase ceramics. Biomaterials. 2000;21(17):1803–10.
15. Webster TJ, Ergun C, Doremus RH, Siegel RW, Bizios R. Specific proteins mediate enhanced osteoblast adhesion on nanophase ceramics. J Biomed Mater Res. 2000;51(3):475–83.
16. Guo X, Gough JE, Xiao P, Liu J, Shen Z. Fabrication of nanostructured hydroxyapatite and analysis of human osteoblastic cellular response. J Biomed Mater Res A. 2007;82(4):1022–32.
17. Li Z, Qu Y, Zhang X, Yang B. Bioactive nano-titania ceramics with biomechanical compatibility prepared by doping with piezoelectric BaTiO(3). Acta Biomater. 2009;5(6):2189–95.
18. Xie XH, Tang TT, Zeng SX, Du RL, Yuan Z, Dai KR. The mechanical properties of bioactive glass/nanohydroxyapatite gradient coatings. J Med Biomech. 2007;22(2):171–6.
19. Du RL, Zeng SX, Hu HY, Xie XH. Hydroxyapatite and bioactive glass composite coating on Ti–6Al–4 V. Bioceramics. 2006;19:589–92.
20. Xie XH, Tang TT, Zeng SX, Du RL, Yuan Z, Dai KR. Biocompatibility of the gradient coating composed of bioactive glass and nanohydroxyapatite. Chin J Biomed Eng. 2007;13(3):156–9.
21. Yamada K, Imamura K, Itoh H, Iwata H, Maruno S. Bone bonding behavior of the hydroxyapatite containing glass-titanium composite prepared by the Cullet method. Biomaterials. 2001;22(16):2207–14.
22. Allegrini S Jr, Rumpel E, Kauschke E, Fanghanel J, Konig B Jr. Hydroxyapatite grafting promotes new bone formation and osteointegration of smooth titanium implants. Ann Anat. 2006;188(2):143–51.
23. Guglielmotti MB, Renou S, Cabrini RL. A histomorphometric study of tissue interface by laminar implant test in rats. Int J Oral Maxillofac Implants. 1999;14(4):565–70.
24. Bauer TW, Geesink RC, Zimmerman R, McMahon JT. Hydroxyapatite-coated femoral stems. Histological analysis of components retrieved at autopsy. J Bone Joint Surg Am. 1991;73(10):1439–52.
25. Klein CP, Patka P, Wolke JG, De Blieck-Hogervorst JM, De Groot K. Long-term in vivo study of plasma-sprayed coatings on titanium alloys of tetracalcium phosphate, hydroxyapatite and alpha-tricalcium phosphate. Biomaterials. 1994;15(2):146–50.
26. Soballe K, Hansen ES, Brockstedt-Rasmussen H, Hjortdal VE, Juhl GI, Pedersen CM, et al. Gap healing enhanced by hydroxyapatite coating in dogs. Clin Orthop Relat Res 1991 Nov;(272):300–7.
27. Rokkum M, Reigstad A, Johansson CB. HA particles can be released from well-fixed HA-coated stems: histopathology of biopsies from 20 hips 2–8 years after implantation. Acta Orthop Scand. 2002;73(3):298–306.
28. Wheeler SL. Eight-year clinical retrospective study of titanium plasma-sprayed and hydroxyapatite-coated cylinder implants. Int J Oral Maxillofac Implants. 1996;11(3):340–50.
29. Zheng X, Huang M, Ding C. Bond strength of plasma-sprayed hydroxyapatite/Ti composite coatings. Biomaterials. 2000;21(8):841–9.
30. Crawford GA, Chawla N, Das K, Bose S, Bandyopadhyay A. Microstructure and deformation behavior of biocompatible TiO_2 nanotubes on titanium substrate. Acta Biomater. 2007;3(3):359–67.
31. Chou BY, Chang E. Plasma-sprayed zirconia bond coat as an intermediate layer for hydroxyapatite coating on titanium alloy substrate. J Mater Sci. 2002;13(6):589–95.
32. Vamsi Krishna B, Xue W, Bose S, Bandyopadhyay A. Functionally graded Co–Cr–Mo coating on Ti–6Al–4 V alloy structures. Acta Biomater. 2008;4(3):697–706.
33. Goyenvalle E, Aguado E, Nguyen JM, Passuti N, Le Guehennec L, Layrolle P, et al. Osteointegration of femoral stem prostheses with a bilayered calcium phosphate coating. Biomaterials. 2006;27(7):1119–28.
34. Ning CY, Wang YJ, Lu WW, Qiu QX, Lam RW, Chen XF, et al. Nano-structural bioactive gradient coating fabricated by computer controlled plasma-spraying technology. J Mater Sci. 2006;17(10):875–84.
35. Chen F, Lam WM, Lin CJ, Qiu GX, Wu ZH, Luk KD, et al. Biocompatibility of electrophoretical deposition of nanostructured hydroxyapatite coating on roughen titanium surface: in vitro evaluation using mesenchymal stem cells. J Biomed Mater Res B Appl Biomater. 2007;82(1):183–91.
36. Gutwein LG, Webster TJ. Increased viable osteoblast density in the presence of nanophase compared to conventional alumina and titania particles. Biomaterials. 2004;25(18):4175–83.
37. Li P. Biomimetic nano-apatite coating capable of promoting bone ingrowth. J Biomed Mater Res A. 2003;66(1):79–85.
38. Lewandrowski KU, Bondre SP, Wise DL, Trantolo DJ. Enhanced bioactivity of a poly(propylene fumarate) bone graft substitute by augmentation with nanohydroxyapatite. Biomed Mater Eng. 2003;13(2):115–24.

39. Han YJ, Loo SC, Lee J, Ma J. Investigation of the bioactivity and biocompatibility of different glass interfaces with hydroxyapatite, fluorohydroxyapatite and 58S bioactive glass. Biofactors. 2007; 30(4):205–16.
40. Gupta R, Kumar A. Bioactive materials for biomedical applications using sol-gel technology. Biomed Mater. 2008;3(3):034005.
41. Jones JR, Tsigkou O, Coates EE, Stevens MM, Polak JM, Hench LL. Extracellular matrix formation and mineralization on a phosphate-free porous bioactive glass scaffold using primary human osteoblast (HOB) cells. Biomaterials. 2007;28(9):1653–63.
42. Hench LL, Polak JM. Third-generation biomedical materials. Science. 2002;295(5557):1014–7.
43. Xynos ID, Edgar AJ, Buttery LD, Hench LL, Polak JM. Ionic products of bioactive glass dissolution increase proliferation of human osteoblasts and induce insulin-like growth factor II mRNA expression and protein synthesis. Biochem Biophys Res Commun. 2000;276(2):461–5.
44. Gao T, Aro HT, Ylanen H, Vuorio E. Silica-based bioactive glasses modulate expression of bone morphogenetic protein-2 mRNA in Saos-2 osteoblasts in vitro. Biomaterials. 2001;22(12): 1475–83.
45. Huiskes R, Weinans H, van Rietbergen B. The relationship between stress shielding and bone resorption around total hip stems and the effects of flexible materials. Clin Orthop Relat Res 1992 Jan;(274):124-34.
46. Chamay A, Tschantz P. Mechanical influences in bone remodeling experimental research on Wolff's law. J Biomech. 1972; 5(2):173–80.
47. Eberhardt C, Habermann B, Muller S, Schwarz M, Bauss F, Kurth AH. The bisphosphonate ibandronate accelerates osteointegration of hydroxyapatite-coated cementless implants in an animal model. J Orthop Sci. 2007;12(1):61–6.
48. Stewart M, Welter JF, Goldberg VM. Effect of hydroxyapatite/tricalcium-phosphate coating on osteointegration of plasma-sprayed titanium alloy implants. J Biomed Mater Res A. 2004; 69(1):1–10.